

Temporal fluctuations of fluorescence resonance energy transfer between two dyes conjugated to a single protein

Taekjip Ha^{a,*}, Alice Y. Ting^b, Joy Liang^a, Ashok A. Deniz, Daniel S. Chemla^{a,c}, Peter G. Schultz^{b,d}, Shimon Weiss^{a,d}

^a *Materials Sciences Division, Lawrence Berkeley National Laboratory, Berkeley, CA 94720, USA*

^b *Howard Hughes Medical Institute, Department of Chemistry, University of California at Berkeley, Berkeley, CA 94720, USA*

^c *Department of Physics, University of California at Berkeley, Berkeley, CA 94720, USA*

^d *Physical Biosciences Division, Lawrence Berkeley National Laboratory, Berkeley, CA 94720, USA*

Received 1 April 1999

Abstract

Biological molecules together with available labeling chemistries provide an ideal setting to investigate the interaction between two closely spaced dye molecules. The photo-excitation of a donor molecule can be non-radiatively transferred to a near-by acceptor molecule via the induced-dipole–induced-dipole interaction in a distance-dependent manner. In this work, we further elaborate on single-molecule fluorescence resonance energy transfer measurements between two dye molecules attached to a *single protein* – staphylococcal nuclease molecules [T. Ha, A.Y. Ting, J. Liang, W.B. Caldwell, A.A. Deniz, D.S. Chemla, P.G. Schultz, S. Weiss, Proc. Natl. Acad. Sci. USA 96 (1999) 893–898]. Temporal fluctuations in the energy transfer signal include: (1) reversible transitions to dark states; (2) irreversible photodestruction; (3) intersystem crossing to and from the triplet state; (4) spectral fluctuations; (5) rotational dynamics of the dyes; and (6) distance changes between the two dyes. To extract biologically relevant information from such measurements, an experimental strategy and data analysis schemes are developed. First, abrupt photophysical events, such as (1)–(3) are identified and removed from the data. The remaining slow, gradual fluctuations in the energy transfer signal are due to spectral shifts, rotational dynamics and distance changes of the dyes. Direct measurements of each dye’s spectral fluctuation and rotational dynamics indicate that these, by themselves, cannot fully account for the observed energy transfer fluctuations. It is therefore concluded that inter-dye distance changes must be present as well. The distance and orientational dynamics are shown to be dependent on the binding of the active-site inhibitor (deoxythymidine diphosphate) to the protein. The inhibitor most probably affects the protein’s stability and the dye–protein interaction, possibly by amplifying the motion of the linker arm between the fluorophore and the protein. © 1999 Elsevier Science B.V. All rights reserved.

1. Introduction

The term single-molecule spectroscopy (SMS) has been recently used to designate the investigation of

optical (usually fluorescence) properties of individual molecules. Because only one molecule is studied at a time, SMS is free from ensemble averaging and allows one to test and compare microscopic theories with experiments. SMS studies of recent years have taught us that fluorescence properties of single molecules are very sensitive to the immediate local

* Corresponding author. Present address: Department of Physics, Stanford University, Stanford, CA 94305, USA.

surroundings [1,2]. Their emissions undergo rich dynamical fluctuations, due to unknown changes in the environment, such as transitions to dark states and spectral shifts. Most of these phenomena are hidden in conventional ensemble measurements and can be unraveled only by SMS.

The introduction of a second, test molecule, which acts as an ‘artificial dominant environment’ can affect the first molecule’s emission properties in a dramatic way. When two fluorescent molecules are brought in close proximity and are optically excited, they can couple and exchange energy via interactions such as induced-dipole–induced-dipole (Förster), higher-order multipoles, electron exchange (Dexter) and spin–spin interactions. SMS of molecular pairs can therefore be used to study such interactions. Moreover, SMS can provide not only information on the interactions themselves, but can also give new insights into the properties of individual molecules. For example, ‘blinking’, routinely used to denote the reversible transition to a non-fluorescent state [3], has been seen on many single-molecular systems [4–9]. These experiments, however, did not reveal the exact nature of the non-fluorescent state, for example, is it a non-absorbing or a zero-quantum yield state? As shown below, SMS on a single-molecular pair decisively answers this question.

Positioning, by physical means, two molecules in close proximity to each other but far away from other pairs can be very challenging. The use of biological macromolecules with relatively well-defined conformations such as proteins, DNAs and RNAs together with biochemical conjugation techniques provide convenient ways to construct such test systems for the study of pair interactions. Moreover, the same close-range interactions can be used to study the macromolecules themselves. Recently, Förster-type fluorescence resonance energy transfer (FRET) between a single donor molecule and a single acceptor molecule was demonstrated [10] and applied for the study of single biomolecules under physiological conditions [11–13].

The great promise of single-pair FRET (spFRET) is in its ability to monitor dynamic structural changes. To become a reliable and widely used technique, a detailed understanding of the transfer mechanism and the photophysical properties of the conjugated fluorophores must be gained on the single-molecule

level. The detailed knowledge of these phenomena will allow the researcher to separate-out photophysical fluctuations from relevant biological information. In this work, spFRET measurements of donor–acceptor labeled proteins under physiological conditions are presented. Various SMS measurements and data analysis schemes are developed and used to separate-out rich molecular pair photophysical effects from biologically relevant distance fluctuations due to slow (millisecond) protein dynamics.

2. Single-pair FRET

In FRET measurements, two points of interest are labeled with different dyes, donor and acceptor. When the acceptor’s absorption spectrum overlaps with the emission spectrum of the donor, and the two dyes are brought into close proximity (2–8 nm), donor energy can be transferred non-radiatively to the acceptor via induced-dipole–induced-dipole interaction with a rate k_t that is inversely proportional to the sixth power of the distance between the two fluorophores. The decay rate of decay of the donor’s excited state is the sum of all decay pathways: $k_r + k_{nr} + k_t$, where k_r is the radiative decay rate and k_{nr} is the sum of all other non-radiative decay rates. The fraction of the donor excitation that is transferred to the acceptor, or the energy transfer efficiency, E , is given by:

$$E = k_t / (k_t + k_r + k_{nr}) = 1 / [1 + (R/R_0)^6], \quad (1)$$

where R is the distance between the donor and acceptor and R_0 is the distance at which 50% of the energy is transferred (Förster radius), and is a function of the properties of the dyes:

$$R_0 = (8.79 \times 10^{-5} n^{-4} \phi_D J \kappa^2)^{1/6} (\text{\AA}). \quad (2)$$

n is the index of refraction of the medium, ϕ_D is the donor quantum yield, J is the spectral overlap of donor emission and acceptor absorption in $\text{nm}^4 \text{M}^{-1} \text{cm}^{-1}$ units, and κ^2 is the relative orientation factor of the two dipoles:

$$\kappa^2 = (\cos \theta_{DA} - 3 \cos \theta_{DR} \cos \theta_{AR})^2, \quad (3)$$

with θ_{DA} the angle between the donor dipole moment, $\vec{\mu}_D$, and the acceptor dipole moment, $\vec{\mu}_A$

. θ_{DR} is the angle between

$\vec{\mu}_{\text{D}}$

and

\vec{R}

(the radius vector between the two dyes), and θ_{AR} is the angle between

$\vec{\mu}_{\text{A}}$

and

\vec{R}

. With no a-priori knowledge of these angles, $0 < \kappa^2 < 4$, presenting a large uncertainty in the determination of R_0 and therefore of R . It is commonly assumed that the two dyes are freely rotating on a time scale faster than the fluorescence lifetime. Under this assumption the orientational factor can be averaged to yield $\kappa^2 = 2/3$ [14].

The importance of Eqs. (1)–(3) is that energy transfer can be used as a *spectroscopic ruler*, as was first convincingly shown by Stryer and Haugland [15], i.e. one can determine distances by measuring the extent of energy transfer (assuming that R_0 is known). Subsequently, FRET has found extensive applications in biological sciences because of its ability to provide information on biomolecular distance scale for in-vitro and in-vivo conditions.

The first demonstration of FRET on a single-molecule level (spFRET) used a DNA construct with dyes attached at each end of the molecule. Energy transfer efficiency was measured from the acceptor's photobleaching dynamics [10]. This measurement used near-field excitation and emission spectroscopy detection, with time resolution limited to seconds. Also, in this early experiment, the DNA was non-specifically laid down on a dry surface with the integrity of the DNA molecule and the relative coordinates between the two dyes being uncertain. More recently, spFRET measurements of freely diffusing DNA constructs with variable donor–acceptor spacing confirmed the distance dependence predicted by Förster theory on the single-molecule level [11–13].

In the work presented here, a few improvements for spFRET measurements are presented: (1) measurements are done under physiological conditions with macromolecules immobilized at the glass–water

interface; (2) specific immobilization and aqueous environment help maintain the integrity of the macromolecules; (3) the time resolution is improved to the millisecond range by the use of far-field excitation (confocal geometry), allowing stronger excitation than possible with the near-field probe and by splitting the two integrated emissions with a dichroic mirror and detecting them using two Avalanche photodiodes (APDs); and (4) a better choice of dyes, allowing better separation between donor and acceptor emissions, while still maintaining large R_0 .

During this work, it was found that dyes were attached to protein molecules display far richer dynamics than when they are conjugated to DNA molecules. Various temporal fluctuations in donor and acceptor intensities were detected. Some were due to discrete dye photophysical events (not related to pair photophysics), such as photobleaching, blinking and triplet states. Others were due to the changes in one or more factors that affect the energy transfer process itself: the distance R , donor and/or acceptor spectrum and hence their overlap integral J , donor and/or acceptor dipole reorientation and hence κ^2 , and quantum yields of the dyes and hence the Förster radius.

To better understand the factors contributing to donor and acceptor emission fluctuations, a series of control experiments were done: spectral fluctuations and rotational dynamics were measured for each dye separately. Spectral fluctuations are found to be negligible. Rotational dynamics are determined to be negligible for the donor but significant for the acceptor. However, these dipole fluctuations cannot account for the large and gradual energy transfer efficiency fluctuations that are observed. It is therefore concluded that distance fluctuations are indeed measured. Contributions from protein conformational dynamics and their dependence on inhibitor binding [11] are also discussed.

3. Experiment

Staphylococcal nuclease (SNase) molecules were labeled with tetramethylrhodamine (TMR) as the donor molecule and with Cy5 as the acceptor

molecule [11]. Donor labeling reaction was done first and was specific to the a single cysteine residue in position 28 (introduced by site-directed mutagenesis) of the amino-acid chain in the protein. Acceptor labeling was performed using an amine-reactive dye and was non-specific in position due to the presence of multiple amines in the protein. The yield of the acceptor's conjugation reaction was intentionally kept low. Only 15–20% of the proteins were labeled with acceptor, consequently reducing the probability for multiple acceptor labeling of one protein. The protein molecules also had an artificial extension of six-histidines at the carboxyl end, aiding the specific immobilization to the nickel-derivatized surface of a glass coverslip [11].

R_0 , calculated from the known spectral properties of the dyes (assuming $\kappa^2 = 2/3$), is 53 Å. Since the protein's diameter is ~ 40 Å, high degree of energy transfer ($E > 70\%$) is expected regardless of the acceptor's position on the protein (lower transfer efficiencies were also observed on the single-molecule level. See results and discussion below). The two dyes emission peaks are separated by 100 nm (570 nm for TMR vs. 670 nm for Cy5) warranting a clear separation by a dichroic beam splitter with very little cross talk. With the filter combinations used (see below), there was no spilling of acceptor signal into the donor detector while only 10% of the donor signal leaked into the acceptor. Furthermore, the absorption of Cy5 at the laser excitation wavelength (514 nm) was 1/50 of its peak absorption, ensuring negligible direct excitation of the acceptor. To enhance the photobleaching lifetimes of the fluorophores, an oxygen scavenging system was used [16].

These spectral properties ensure that in a single pair experiment, the signal at the donor detector, I_d , is proportional to the true donor intensity I_{d0} , and the signal at the acceptor detector, I_a , is directly proportional to the true sensitized acceptor intensity (energy transferred from donor) I_{a0} . The proportionality constants η_a and η_d are dependent on the detection efficiency of each molecule through the optical system. It is shown in the results section that the energy transfer efficiency can be determined from the measured I_d and I_a .

Proteins were immobilized on the glass–water interface with low areal density such that only one molecule was under the laser excitation volume at a

time. Laser light (514 nm Ar ion laser, 15 μ W, circularly polarized) was focused to a 0.4 μ m spot using an oil immersion objective (Zeiss, Plan-Apochromat, NA = 1.4) in an epi-illumination geometry of a home-made scanning-stage confocal microscope. The fluorescence emission was collected by the same objective and divided into two by a dichroic beam splitter (long pass at 630 nm) and detected by two APD counting units (EG & G Canada, SPCM-200). A 585 nm band pass filter was placed in front of the donor detector; a 650 nm long pass filter was placed in front of the acceptor detector. Since fluorescence detection spectral ranges are sufficiently removed from the cutoff wavelength of the dichroic beam splitter, the polarization dependence of the detection efficiency of both donor and acceptor signal is negligible in our system. As shown elsewhere [17], the polarization mixing due to the high NA objective can also be neglected here.

To acquire donor and acceptor emission time records, an automatic search, conditioned on the acceptor signal, was employed [18]. This conditioning aided the screening for doubly labeled proteins: with no direct excitation of the acceptor, only molecules experiencing FRET could show acceptor signal. Once a protein was screened, located and positioned under the laser spot, donor and acceptor time traces (5 ms integration time) were acquired. The acquisition lasted until both molecules photobleached. Using the oxygen scavenging system, typical time traces lasted for a few seconds.

Donor-only labeled proteins were used to study spectral fluctuations of the donor. To separate out dipole fluctuations from spectral shifts, the emission was first passed through a band pass filter (matching the donor emission), then through an analyzer which selected only one polarization state. Lastly, the emission was split by a dichroic beam splitter (570 nm long pass). The role of the analyzer was to bypass the polarization-dependent transmission of the dichroic mirror. Acceptor spectral fluctuations were measured in a similar way on doubly-labeled proteins by directly exciting Cy5 with the 633 nm HeNe laser line. The two-halves of the donor (acceptor) emission were recorded using the two APDs as in spFRET measurements.

Donor rotational dynamics was studied by recording the excitation/emission polarization response of

donor-only labeled proteins. The laser excitation polarization was alternated between two orthogonal linear polarization states every consecutive data point using an electro-optic modulator (ConOptics, M350). The emission was first passed through a band pass filter (matching the donor emission) and then split by a broadband polarizing beam splitting cube into two orthogonally polarized components which were detected by the two APDs. Acceptor rotational dynamics was measured on the doubly-labeled proteins in a similar way using the 633 nm HeNe laser line.

4. Results and discussions

Fig. 1 shows typical donor and acceptor time traces measured for a single, doubly-labeled protein. As can be seen, the acceptor signal is strong most of the time while the donor signal is quenched, indicating high energy transfer efficiency ($E > 0.9$). About 30 out of the 100 molecules studied showed similar time traces. The very high transfer efficiency is most probably due to the short distance (compared to

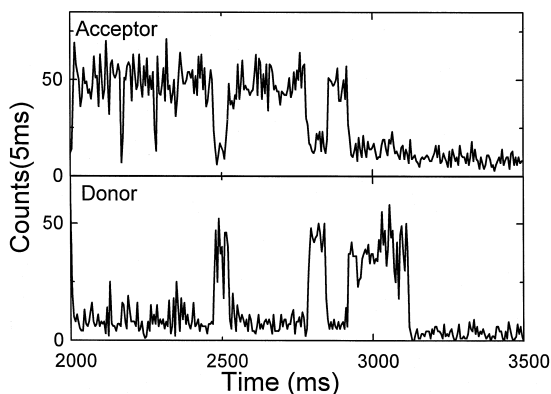


Fig. 1. Time traces of acceptor (top) and donor (bottom) intensities measured on a single inhibitor-free protein specifically immobilized to the surface. Acceptor strongly emits due to the near complete energy transfer from the donor. Blinking events occasionally interrupt its emission. During acceptor's blinking, donor signal is increases because it can not lose energy anymore to the acceptor. When the acceptor resumes its mission, the donor signal is again decreased to its original low level. Two anticorrelated blinking events occurred at ~ 2500 and ~ 2800 ms. The third and final anticorrelated change happened due to the permanent photobleaching of the acceptor at 2900 ms, followed by the photobleaching of the donor at 3100 ms.

Förster radius) between the two dyes. At such short distances, the pair emission is mostly sensitive to discrete photophysical events. In the figure, the acceptor signal suddenly decreases to the background level at ~ 2500 ms, but comes back to its original level 50 ms later. Similar 'blinking' events were also observed for donor-only and acceptor-only labeled proteins.

Blinking has been document for a variety of systems such as dyes [4,5], photosynthetic systems [7], fluorescent proteins [6] and nanocrystals [8]. It is directly observed only by SMS and therefore often used as an evidence for the single-molecule origin of the signal. However, even multi-chromophoric systems such as conjugated polymers were shown to blink [9].

Until now, the exact nature of the non-fluorescent state was not known. Is it due to a non-absorbing state, or is it the result of a zero (emission) quantum yield state? Since it is very difficult, if not impossible, to directly measure the absorption (and therefore the quantum yield) of a single molecule, this question could not have been answered. It is shown here that the induced-dipole–induced-dipole interaction of a single-molecular pair provides a way to indirectly measure single-molecule absorption, hence conclusively answering the above question. In Fig. 1, coincident with the acceptor blinking, a momentary surge in the donor signal is observed. It may be argued that this surge could be a result of a sudden distance or orientational change, but such effects would not happen in an all-or-nothing manner as is shown here. In addition, blinking of similar frequency was observed from acceptor-only samples. We therefore contend that the anti-correlated surge indicates that acceptor's non-fluorescent state is non-absorbing. The donor was transferring all of its excitation to the acceptor prior to the blinking event. During blinking, it cannot transfer anymore energy to the non-absorbing state of the acceptor. Once the acceptor returns to its emitting state, the donor signal is quenched again. Second anti-correlated donor–acceptor emissions due to the acceptor blinking are seen at 2800 ms. When the donor blinks, on the other hand, both donor and acceptor signal disappear (data not shown). The induced-dipole–induced-dipole interaction could also elucidate the much debated nature of emission intermittency of semiconductor nanocrystals [8,19].

Another abrupt photophysical event is the photo-destruction, or photobleaching, of the fluorophore. That is, after a typical excitation and emission cycles, excited molecules permanently switch to a non-emitting state. In Fig. 1, the acceptor molecule photobleached at 2900 ms, accompanied by a sudden increase in the donor signal. This indicates that the acceptor photobleached product is non-absorbing as in the case of blinking. Eventually, the donor molecule photobleached as well at 3100 ms.

The amount of donor signal recovery upon acceptor photobleaching is related to the quantum yields of the molecules (ϕ_d and ϕ_a) and their overall detection efficiencies (η_d and η_a). It can be easily shown that γ ($\equiv \eta_a \phi_a / \eta_d \phi_d$) is equivalent to $|\Delta I_a / \Delta I_d|$, where ΔI_a and ΔI_d are the acceptor and donor intensity changes, respectively, upon acceptor photobleaching. $|\Delta I_a / \Delta I_d|$ was determined from 45 acceptor photobleaching events, and its distribution was centered at 0.8. Later, this γ value we will be used to determine energy transfer efficiency from donor and acceptor intensities.

A third abrupt photophysical phenomena, composed of short (millisecond) ‘spikes’ in donor and acceptor intensities is also displayed in Fig. 1. Two spikes at 2160 and 2280 ms are clearly resolved for the acceptor channel. Spikes in the donor channel are less pronounced. These spikes most likely manifest transitions to and from the triplet state [20]. Fig. 2 shows such short transitions more clearly. As in the case of blinking, donor and acceptor spikes are anti-correlated: momentary drops in the acceptor emission are accompanied by simultaneous increases in donor signal. The drops in the acceptor signal are often shorter than the integration time (5 ms) and therefore not fully resolved. On the single-molecule level, triplet states were first observed indirectly, through fluorescence bunching, as revealed by the autocorrelation of the emission intensity fluctuations [21]. Later, they were directly detected as discrete quantum jumps in the emission [22]. In an oxygen deficient system, the dye’s triplet state lifetime can be elongated to the milliseconds range. Under such conditions, room-temperature fluorescence time traces display telegraph-noise like short dark periods in the emission each time the dye is shelved in the triplet state [20]. This rapid blinking behavior is distinct from the slower blinking discussed before.

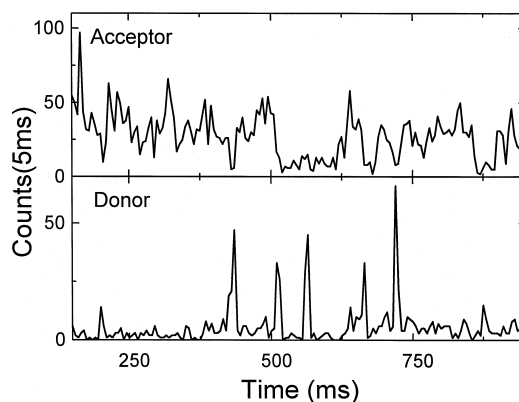


Fig. 2. Time traces of acceptor (top) and donor (bottom) intensities measured on a single inhibitor-free protein. The donor signal momentarily surges several times due to the acceptor’s transition to the triplet state. During these transitions the donor can not lose energy to the acceptor and therefore its emission spikes up. The spikes occur only when the acceptor signal is low.

They are much more frequent and much shorter in duration. In the current measurement (Figs. 1 and 2), the time resolution is not fast enough to fully resolve individual transitions to the triplet state. Yet, some of the longer transitions are visible in the form of sharp anticorrelated spikes. The spikes are not visible when the oxygen scavenging system is not used, supporting their triplet state origin.

The above measurements suggest an intriguing possibility for studying cooperative quantum jumps of two molecules. Intersystem crossing to and from the triplet state has a relatively slow rate (microseconds to milliseconds) because it involves a forbidden transition which requires a change in the spin state of the molecule. Using a DNA (or another macromolecule) construct with two very closely spaced (few Å) fluorophores might allow one to observe cooperative intersystem crossing transitions in a way that will conserve the total spin of the system. Similar cooperative quantum jumps have been measured for single ions in radio frequency traps [23].

Once the origins of blinking, photobleaching and triplet state spikes were determined, the following analysis was employed to discount their effects such that other factors contributing to the temporal fluctuations of energy transfer could be further investigated. After subtracting the background signal from donor and acceptor time traces a median filter with

five points average was applied to remove triplet spikes. Next, data points that showed simultaneous dark counts on both detectors due to donor blinking events were disregarded from the time traces.

Energy transfer efficiency time trace was then obtained by using the relation: $E(t) = [1 + I_d^0 \phi_a / I_a^0 \phi_d]^{-1}$, where I_d^0 and I_a^0 are the true donor intensity and the true sensitized acceptor emission, respectively. I_d^0 and I_a^0 are related to the measured intensities I_d and I_a by proportionality factors of η_d and η_a that account for the overall instrument detection efficiencies for both fluorophores. Therefore, E can be written as: $E(t) = [1 + \gamma I_d / I_a]^{-1}$ with a correction factor γ as defined above (determined to be 0.8). It is emphasized that this analysis is valid only when the direct excitation of the acceptor and the donor leakage into the acceptor channel are negligible, such that I_a can be considered to originate entirely from the energy transfer process. Once $E(t)$ was determined, its \bar{E} and its autocorrelation function $G_E(t)$ were calculated. Data points with $E < 0.3$ were excluded to disregard acceptor blinking events. $G_E(\tau)$ for $\tau > 0$ was then fit to: $f(\tau) = a_E^2 \exp(-\tau/\tau_E)$ and the fluctuations amplitude, a_E , and time scale, τ_E , were extracted. It is noted that the shot noise contribution to the fluctuations is automatically discarded by the autocorrelation function while the temporally correlated fluctuations are retained.

Representative donor and acceptor time traces from a single protein molecule together with the above analysis are shown in Fig. 3. Only a section of the full time traces that does not show blinking was chosen. Both acceptor and donor signals display significant and gradual fluctuations (Fig. 3a and b). The calculated $E(t)$ fluctuations (Fig. 3c) drop below $E = 0.5$ several times, a too low transfer efficiency value for a maximum separation of 40 Å (protein diameter) between the two dyes. In fact, only 48 protein molecules (out of 100) showed time-averaged transfer efficiency of $84\% < \bar{E} < 100\%$ with presumed donor–acceptor distances smaller than 40 Å. 52 molecules displayed too low \bar{E} values between $45\% < \bar{E} < 84\%$. These discrepancies suggests that either many protein molecules were denatured, or that R_0 , a concept that was developed for ensemble FRET measurements, is a mere parameter of convenience and should not be

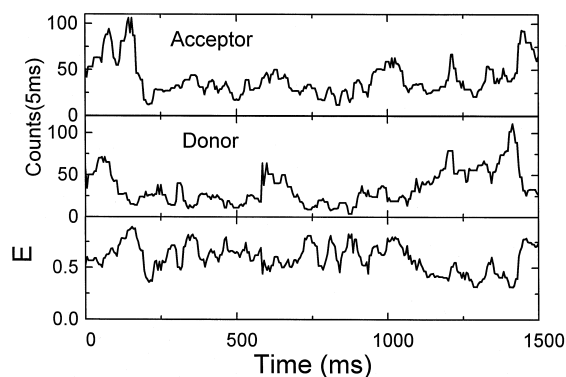


Fig. 3. Time traces of acceptor (top) and donor (middle) intensities measured on a single inhibitor-free protein. A median filter was applied to reduce the noise caused by triplet states. There are large and gradual fluctuations in I_d and I_a that occur over tens of milliseconds. The FRET efficiency time trace (bottom) is calculated from $E(t) = [1 + \gamma I_d / I_a]^{-1}$ (see text).

taken on its face value for the analysis of spFRET experiments. Because of local environment effects, R_0 can change from molecule to molecule or even vary in time for a particular molecule due to alterations in molecular parameters. It is therefore concluded that $E(t)$ fluctuations can be caused either by changes in the distance R , or by changes in R_0 , according to: $E(t) = [1 + \{R(t)/R_0(t)\}^6]^{-1}$. As demonstrated below, one of the main contributors to R_0 fluctuations is the orientational factor κ^2 .

R_0 depends on the spectrum of the two dyes, the donor quantum yield and the relative orientation of the two dipoles. TMR spectral fluctuations were separately studied on donor-only labeled proteins. Cy5 spectral fluctuations were studied on doubly labeled proteins by exciting the acceptor with the HeNe laser. In each case, the fluorophore's emission was split into two components with a dichroic beam splitter centered at the peak emission of the dye. The short- and long-wavelength components were measured separately using the two APD detectors.

Cy5 representative spectral traces are shown in Fig. 4. Both short- and long-wavelength components fluctuate together through multiple blinking and spikes without any noticeable change in their relative ratio. Similar results were obtained for TMR. From such measurements, an upper limit of 2–3 nm can be placed on donor and acceptor spectral shifts. Such low values insignificantly affect the spectral overlap

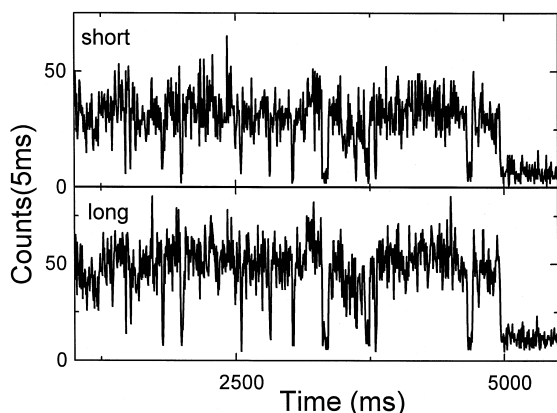


Fig. 4. Acceptor's spectral time traces detected at the short-wavelength detector (top) and long-wavelength detector (bottom) on a single inhibitor-free doubly-labeled protein. The 633 nm line of a HeNe laser directly excited the acceptor. The emission was split into two by a dichroic beam splitter. Both traces show correlated fluctuations with little change in their ratio.

J (donor emission spectrum and acceptor absorption spectrum are both broader than 530 nm).

The donor quantum yield, which is also included in the expression for R_0 (Eq. (2)), cannot be determined for a single molecule because its absorption cannot be measured. However, as we will conclude from the rotational dynamics analysis presented below, donor's intensity fluctuations other than blinking are mainly caused by its rotational dynamics.

Rotational dynamics of each dye were measured by alternating the laser linear excitation polarization between two orthogonal directions, s and p while analyzing (with a polarizing beam splitting cube) and measuring the two emission components on two detectors, I_s and I_p . The s and p axes are defined relative to the cube. Fig. 5a shows a single-donor signal measured on a protein labeled with TMR only. Both I_s and I_p show periodic fluctuations (with a period of two consecutive data points) resulting from the successive alternation of the excitation polarization. I_s and I_p are generally anticorrelated. When their intensities are averaged for each two consecutive data points (as if the excitation was with a circularly polarized light), they display similar average intensities.

As previously shown [24], such behavior indicates a relatively unhindered and rapid rotation of the dye. When a dipole is rotating much faster than the data

acquisition time, a dynamic photoselection process gives rise to the anticorrelated relationship between I_s and I_p . During its rotation, the dye is preferentially excited when its dipole is aligned with the instantaneous laser polarization. If the rotational diffusion during the excited state lifetime is insignificant, the emission will also be mostly polarized along the laser polarization. Therefore, s -polarized laser excitation will result in a much stronger signal on the I_s detector, while p -polarized light will produce a stronger signal on the I_p detector, and hence anticorrelation dependence between the two.

The modulation depth of these signals contains information on the rotational diffusion time scale. The data points in Fig. 5 can be written as I_{ij} , with the first index denoting the emission (analyzed) polarization and the second index denoting the excitation polarization. It can be shown that $I_{ss}/I_{sp} = I_{pp}/I_{ps} = 3$ for an unhindered rotation with a time scale slower than the excited state lifetime (assuming that the absorption and emission transition dipoles are parallel). The data in Fig. 5a show a modulation depth with a I_{ss}/I_{sp} ratio that is smaller than 2, suggesting a significant depolarization, and therefore sub-nanosecond rotational diffusion during the excited state lifetime.

To quantify the rotational fluctuations of the dye, effective average dipole angle parameter $\theta_{em}(t)$ is defined in the following way:

$$\theta_{em}(t) = \tan^{-1} \left[\frac{I_{sp}(n) + I_{ss}(n)}{\{I_{ps}(n+1) + I_{pp}(n+1)\}^{0.5}} \right]. \quad (4)$$

I_{ij} are a set of four consecutive data points taken at times n and $n+1$. When $\theta_{em}(n)$ assumes a value of $\theta_{em} \approx 45^\circ$, the dipole is either fixed along the 45° angle (measured from the p axis), or it rapidly rotates with little or no restriction. In contrast to the single-molecule polarization experiments performed by Warshaw et al. [25], the polarization modulation employed here lifts such ambiguity. The anticorrelation behavior in Fig. 5a clearly indicates rapid rotation. A fixed dipole, on the other hand, will show a correlated relationship between the two signals, with the relative intensities at same time (n) points determining the dipole angle: $= \tan^{-1}[I_{sp}(n)/I_{pp}(n)]^{0.5} = \tan^{-1}[I_{ss}(n+1)/I_{ps}(n+1)]^{0.5}$. When $\theta_{em} \gg 45^\circ$ or $\theta_{em} \ll 45^\circ$, individual time points can again indi-

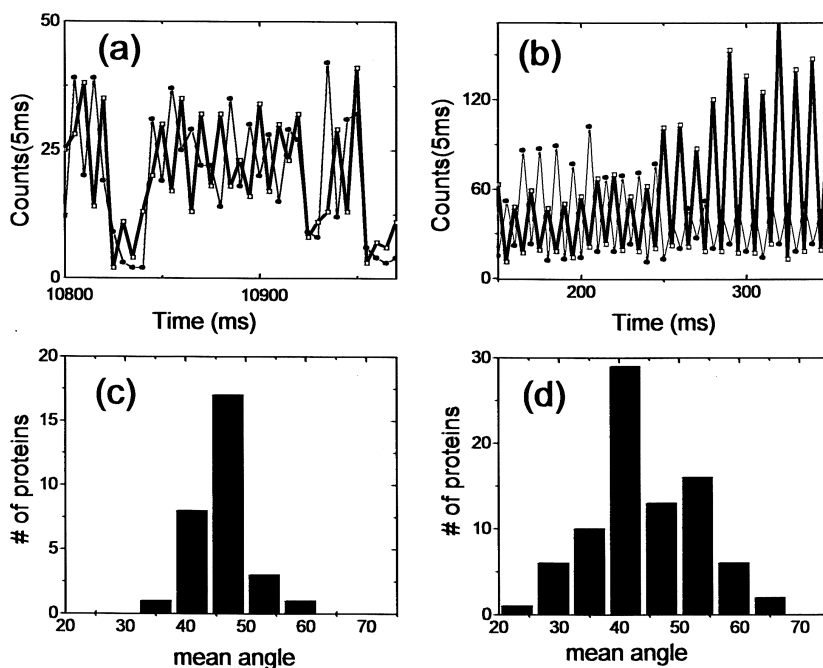


Fig. 5. Polarization responses of single donors attached to inhibitor-free and -bound forms of TMR-only labeled proteins. (a) Donor polarization s and p time trace for an inhibitor-free protein. (b) Donor polarization s and p time trace for an inhibitor-bound protein. The s detector signal, (I_s), is denoted with squares with thick lines; the p detector signal, (I_p), is denoted with circles and thin lines. The laser excitation was alternated between s and p polarizations for every data point. Both (a) and (b) show anticorrelation between I_s and I_p detectors, evidence for rapid rotation of the donor. Inhibitor binding (b) causes an asymmetry in between I_s and I_p (or their ratio) that changes over time. This effect is also shown in the histograms of the angle parameter, $\bar{\theta}$ for the inhibitor-free (c) and the inhibitor-bound (d) proteins (see text).

cate a fixed dipole (at θ_{em} degrees from the p axis). However, consecutive time points in a modulation experiment indicate a rapid rotation of a dipole that is rotationally hindered to a cone. An example is given in Fig. 5b. The data were acquired from a donor-only labeled a protein with its active-site inhibitor bound to it. The entire time trajectory of Fig. 5b shows an anticorrelation relationship between I_s and I_p , indicating rapid rotation. However, the ratio I_{sj}/I_{pj} , and therefore the instantaneous emission angle, slowly fluctuate. This measurement is consistent with a hindered rotational diffusion within a cone whose axis is precessing on a milliseconds time scale. Such rotational fluctuations were not seen from the donor when it was conjugated to the inhibitor-free state of the protein (Fig. 5a). The active-site inhibitor also causes an increase in the modulation depth, indicating a slower time scale for the rotational diffusion.

In a similar way to the analysis of $E(t)$ fluctuations, $\theta_{em}(t)$ was calculated from the raw data, and its time-average, $\bar{\theta}$, and its autocorrelation function, $G_R(\tau)$, were computed. $G_R(\tau)$ for $\tau > 0$ was fit with $a_R^2 \exp(-\tau/\tau_R)$, where a_R and τ_R are the dipole fluctuations amplitude and time scale, respectively. Again, only temporally correlated fluctuations are retained in a_R .

The same polarization modulation data sets were also analyzed for the fluorophore's intensity fluctuation. A time trajectory of the intensity was extracted from the raw data according to: $I(m) = I_{sp}(n) + I_{ss}(n) + I_{ps}(n+1) + I_{pp}(n+1)$ ($n = 2, 4, 6, \dots$ – this operation reduces the data range and the temporal resolution by a factor of 2). Blinking events were excluded from the analysis. Again, the autocorrelation of $I(m)$ was calculated and fit with $a_I^2 \exp(-\tau/\tau_I)$. Although τ_R and τ_I varied over a wide range (10 ms to 1 s) among molecules, their

ratio for individual molecules did not vary by more than a factor of 2. This observation suggests that the intensity fluctuations (excluding blinking and inter-system crossing) are mainly caused by the dye's rotational diffusion, while spectral fluctuations and the changes in quantum yields are negligible.

Fig. 5c shows the distribution of θ measured for single donors attached to inhibitor-free Snase molecules. A narrow distribution, centered at 45° , is evident for the free proteins, implying a relatively unhindered, rapid rotation of the dye. This rotation is severely restricted and becomes highly anisotropic upon inhibitor binding, as can be concluded from the larger $\bar{\theta}$ scatter in Fig. 5d.

Similar measurements were performed on acceptors of doubly-labeled proteins (using the HeNe laser), with and without the inhibitor. Acceptors exhibited considerable rotational fluctuations even in the case of inhibitor-free proteins. The addition of the inhibitor did not change qualitative outcome (data not shown). Since the acceptor labeling was not specific, these results are harder to interpret. Possible explanations might involve acceptor–surface and/or acceptor–protein interactions that produce dipole fluctuations. For example, some acceptors can be attached to sites that are very close to the C-terminus of the protein, where it is anchored to the surface through the histidine tag. Interaction with the surface can greatly perturb the rotational degree of freedom. The donor attachment site (cysteine 28), on the other hand, is $\sim 40 \text{ \AA}$ away from the C-terminus (determined from the crystal structure) so that surface interactions are less likely. In fact, polarization modulation measurements on donor-labeled, inhibitor-free proteins that were non-specifically attached to the surface showed significant rotational fluctuations (data not shown). This observation asserts the importance of specific immobilization that orients the proteins with respect to the interface and therefore reduces the ill effects of dye–surface interactions.

Coming back to the energy transfer fluctuations, the polarization modulation studies now allow us to significantly reduce the uncertainty in κ^2 . The worst case scenario of a fixed acceptor at a random orientation and a freely and rapidly rotating donor automatically limits κ^2 to: $1/3 < \kappa^2 < 4/3$ [26]. This uncertainty contributes to $E(t)$ fluctuations according to: $\Delta E = E(1 - E)\Delta\kappa^2/\kappa^2$. The mean value of the ori-

entational factor, κ^2 , and its distribution width (standard deviation), $\Delta\kappa^2$, were determined by numerical simulations according to the above assumptions. The solid line in Fig. 6a shows this limit, representing the maximum possible contribution of the dyes rotational fluctuations to ΔE . This estimate is a very conservative one because the acceptor is almost never at a really fixed orientation. Therefore, $\Delta\kappa^2$ should have even a narrower range. Also displayed in Fig. 6a is a 2D scatter plot of $E(t)$ fluctuations amplitude, a_E , plotted against the time-

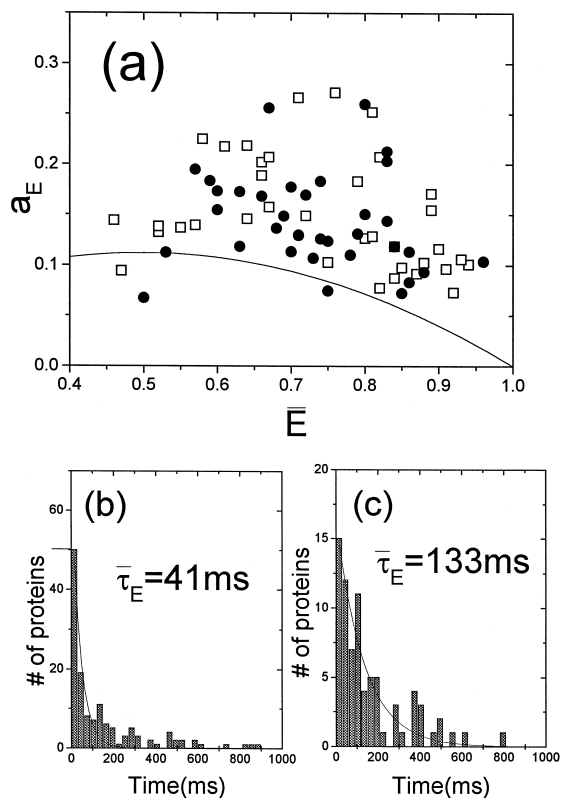


Fig. 6. (a) Scatter plot of $E(t)$ fluctuations amplitude, a_E , vs. the mean energy transfer efficiencies, \bar{E} , for inhibitor-free (empty squares) and inhibitor-bound proteins (filled circles). The scatter in \bar{E} possibly reflects the nonspecific labeling of the acceptor. The solid line represents the maximum possible contribution of acceptor's dipole fluctuations to a_E for inhibitor-free proteins. (b) Histogram of $E(t)$ fluctuation time scales, τ_E , for 100 inhibitor-free proteins. The values range from 10 ms to 1 s, with an average of 41 ms. (c) Histogram of $E(t)$ fluctuation time scales, τ_E , for inhibitor-bound proteins. These time constants are considerably larger (average = 133 ms) than the ones measured for inhibitor-free proteins.

average of $E(t)$, \bar{E} , for free proteins (squares) and inhibitor-bound proteins (circles). Most data points (except for 3) have fluctuations amplitude well above the solid line, suggesting the rotational fluctuations alone cannot account for the observed $E(t)$ fluctuations measured for inhibitor-free proteins.

Since it has been reasoned above that spectral and quantum yield fluctuations are negligible and that rotational fluctuation of the dyes cannot alone explain the fluctuations in the energy transfer efficiency, it is concluded that significant distance fluctuations between the two dyes must be present. This conclusion does not necessarily mean that $E(t)$ fluctuations directly reflect protein conformational dynamics. Because of their tethers, dye reorientations can entail repositioning and changes in their interdistance. In fact, protein conformational dynamics, if present at all, is likely to affect its interactions with the dyes, resulting in the amplification of the tethers movements and dipole reorientations. However, it is possible to infer the contribution of conformational dynamics by comparing $E(t)$ and $\theta_{em}(t)$ fluctuations for the inhibitor-free and -bound states of the protein. The crystal structures of both forms are known and their differences are very subtle. Although the acceptor is non-specifically bound and its location is unknown, it is very unlikely that inhibitor binding will change the static distance between the donor and the acceptor significantly enough to be detected by time-averaged FRET. Fig. 6a shows that indeed both \bar{E} and a_E distributions are essentially the same for the two cases. Nonetheless, statistically significant different $E(t)$ fluctuations time scales, τ_E 's, are detected for the two states of the protein. Fig. 6b and c show τ_E histograms for ~ 100 molecules of inhibitor-free and -bound proteins, respectively. The average values of these distributions are determined by a fit to a single exponent. The $E(t)$ fluctuations of the inhibitor-free protein are roughly 3-fold faster than the fluctuations time scale measured for the inhibitor-bound protein (41 ms vs. 133 ms). Given the number of proteins studied, the probability that this difference is caused by statistical aberrations is very small ($< 0.1\%$). Slower fluctuations time scale suggest that inhibitor binding stabilizes the protein, and supports the notion that $E(t)$ fluctuations indeed report, at least in part, on protein conformation dynamics.

It was shown that inhibitor binding affects the dynamics of the dyes in two ways. First, it induces increased rotational fluctuations of the donor which may be the result of the direct interaction between the dye and the inhibitor. Second, it slows down the fluctuations of energy transfer efficiency. It can be argued that the second observation is a manifestation of the first. However, increased rotational fluctuations of the donor will cause, if at all, faster energy transfer fluctuations upon inhibitor binding, in contrast to what is observed. It is therefore deduced that at least part of the observed $E(t)$ and $\theta_{em}(t)$ fluctuations must be caused by millisecond structural fluctuations of the protein itself. Although the exact mechanism is not known, it is believed that the linker between the protein and the dye (tether) amplifies the protein's structural fluctuations. Using constructs with different length dye tethers might further elucidate these results.

5. Conclusions

A variety of dynamical phenomena were measured using two dyes attached to a single protein. None of these observations could have been made on the ensemble level. This study, therefore, clearly illustrates the power of single-molecule fluorescence spectroscopy. Dye photophysics such as blinking, photobleaching and intersystem crossing to the triplet state affect the FRET signal between the donor and the acceptor in a significant but identifiable way so that their effects could be discounted in a subsequent analysis. It was shown that both rotational dynamics and distance fluctuations cause the remaining fluctuations in the FRET signal. A comparison between the inhibitor-free and -bound forms of the protein suggests that protein conformational dynamics is at the origin of these remaining fluctuations.

Single pair FRET is a powerful technique which has the potential to advance our understanding of the conformational states and dynamics of biological macromolecules in equilibrium, upon ligand binding, during folding and denaturing, or during catalysis, in ways which ensemble methods cannot even address. It is noted that spFRET can be a more powerful technique than single-molecule polarization study of single molecules because the former probes the inter-

nal conformational states in the center-of-mass frame of the system, hence it is less prone to complications due to the overall motion of the macromolecule itself. Nonetheless, using two non-interacting, different dyes, and two excitation beams, it might be possible to measure relative orientational changes between two sites.

The current study uncovers many interesting dynamics of dye photophysics and protein conformational fluctuations. Detailed understanding of the structural changes, however, has not been attained. Non-specific labeling of the acceptor is one reason. SNase being a small globular protein that does not exhibit large conformational changes under the experimental conditions described here is another. The spFRET methodology will be greatly enhanced if dye–protein conjugation chemistries are further improved and developed to allow site-specific labeling of both donor and acceptor. Furthermore, utilizing the technique to the study of macromolecules that display large conformational changes will simplify interpretation of the results. In that case, signal fluctuations due to dye photophysics and linker dynamics can be less significant compared to the changes resulting from large conformational changes. The technique may also prove useful for studying the interaction between two separate biological molecules, one labeled by with a donor, the other with acceptor [11,12]. After all, what other configuration can give rise to larger distance changes than the association and dissociation of two molecules?

Acknowledgements

Financial support for this work was provided by the National Institutes of Health (Grant No. GM49220), by the Laboratory Directed Research and Development Program of Lawrence Berkeley National Laboratory under US Department of Energy, contract No. DE-AC03-76SF00098, and by the Office of Naval Research Contract N0001498F0402. PGS is a Howard Hughes Medical Institute (HHMI) Investigator and a W.M. Keck Foundation Investigator. AYT is supported by an NSF predoctoral fellowship.

References

- [1] W.E. Moerner, *Science* 265 (1994) 46.
- [2] X.S. Xie, J.K. Trautman, *Annu. Rev. Phys. Chem.* 49 (1998) 441.
- [3] W.E. Moerner, *Science* 277 (1997) 1059.
- [4] W.P. Ambrose, P.M. Goodwin, J.C. Martin, R.A. Keller, *Science* 265 (1994) 364.
- [5] T. Ha, T. Enderle, D.S. Chemla, P.R. Selvin, S. Weiss, *Phys. Rev. Lett.* 77 (1996) 3979.
- [6] R.M. Dickson, A.B. Cubitt, R.Y. Tsien, W.E. Moerner, *Nature (London)* 388 (1997) 355.
- [7] M.A. Bopp, Y. Jia, L. Li, R.J. Cogdell, R.M. Hochstrasser, *Proc. Natl. Acad. Sci. USA* 94 (1997) 10630.
- [8] M. Nirmal, B.O. Dabbousi, M.G. Bawendi, J.J. Macklin, J.K. Trautman, T.D. Harris, L.E. Brus, *Nature (London)* 383 (1996) 802.
- [9] D.A. Vandebout, W.T. Yip, D. Hu, D.K. Fu, T.M. Swager, P.F. Barbara, *Science* 277 (1997) 1074.
- [10] T. Ha, T. Enderle, D.F. Ogletree, D.S. Chemla, P.R. Selvin, S. Weiss, *Proc. Natl. Acad. Sci. USA* 93 (1996) 6264.
- [11] T. Ha, A.Y. Ting, J. Liang, W.B. Caldwell, A.A. Deniz, D.S. Chemla, P.G. Schultz, S. Weiss, *Proc. Natl. Acad. Sci. USA* 96 (1999) 893.
- [12] G.J. Schütz, W. Trabesinger, T. Schmidt, *Biophys. J.* 74 (1998) 2223.
- [13] A.A. Deniz, M. Dahan, T. Ha, J. Grunwell, D.S. Chemla, S. Weiss, P.G. Schultz, *Proc. Natl. Acad. Sci. USA* (1999, submitted).
- [14] C.R. Cantor, P.R. Schimmel, *Biophysical Chemistry*, vol. 2. W.H. Freeman, San Francisco, CA, 1980.
- [15] L. Stryer, R.P. Haugland, *Proc. Natl. Acad. Sci. USA* 58 (1967) 719.
- [16] T. Funatsu, Y. Harada, M. Tokunaga, K. Saito, T. Yanagida, *Nature (London)* 374 (1995) 555.
- [17] T. Ha, T.A. Laurence, D.S. Chemla, S. Weiss, *J. Phys. Chem.* (1999, submitted).
- [18] T. Ha, D.S. Chemla, T. Enderle, S. Weiss, *Appl. Phys. Lett.* 70 (1997) 782.
- [19] U. Banin, M. Bruchez, A.P. Alivisatos, T. Ha, S. Weiss, D.S. Chemla, *J. Chem. Phys.* 10 (1999) 1.
- [20] T. Ha, T. Enderle, D.S. Chemla, P.R. Selvin, S. Weiss, *Chem. Phys. Lett.* 271 (1997) 1.
- [21] M. Orrit, J. Bernard, *Phys. Rev. Lett.* 65 (1990) 2716.
- [22] T. Basche, S. Kummer, C. Brauchle, *Nature (London)* 373 (1995) 132.
- [23] T. Sauter, R. Blatt, W. Neuhauser, P.E. Toschek, *Opt. Commun.* 60 (1986) 287.
- [24] T. Ha, J. Glass, T. Enderle, D.S. Chemla, S. Weiss, *Phys. Rev. Lett.* 80 (1998) 2093.
- [25] D.M. Warshaw, E. Hayes, D. Gaffney, A.M. Lauzon, J. Wu, G. Kennedy, K. Trybus, S. Lowey, C. Berger, *Proc. Natl. Acad. Sci. USA* 95 (1998) 8034.
- [26] R.E. Dale, J. Eisinger, W.E. Blumberg, *Biophys. J.* 26 (1979) 161.